(9) J. P. Larkindale and D. J. Simkin, *J. Chem. Phys.*, **55**, 5668 (1971).
(10) R. E. Linder, H. Weiler-Felichenfeld, G. Barth, E. Bunnenberg, and C. Dje-rassi, *Theor. Chim. Acta*, **36**, 135 (1974).
(11) R. E. Linder, E. Bunnenberg, L. Seamans, and A. Moscowitz, *J. Chem. Phys.*, **60**, 1943 (1974).
(12) (a) J. S. Rosenfield, A. Moscowitz, and R. E. Linder, *J. Chem. Phys.*, **61**, 2427 (1974); (b) J. S. Rosenfield, *J. Chem. Phys.*, **66**, 921 (1977).
(13) F. M. Sprinkel, D. D. Shillady, and R. W. Strickland, *J. Am. Chem. Soc.*, **97**, 6653 (1975).
(14) J. S. Rosenfield, *Chem. Phys. Lett.*, **39**, 391 (1976).
(15) J. H. Obbink and A. M. F. Hezemans, *Theor. Chim. Acta*, **43**, 75 (1976).
(16) A. Kaito, M. Hatano, and A. Tajiri, *J. Am. Chem. Soc.*, **99**, 5241 (1977).
(17) (a) J. A. Pople, D. P. Santry, and G. A. Segal, *J. Chem. Phys.*, **43**, S129 (1965); (b) J. A. Pople and G. A. Segal, *ibid.*, **43**, S136 (1965); (c) *ibid.*, **44**, 3289 (1966).
(18) J. Del Bene and H. H. Jaffé, *J. Chem. Phys.*, **48**, 1807 (1968).
(19) J. M. Sichel and M. A. Whitehead, *Theor. Chim. Acta*, **7**, 32 (1967).
(20) N. Mataga and K. Nishimoto, *Z. Phys. Chem. (Frankfurt am Main)*, **12**, 335 (1957).
(21) One of the referees called our attention to the location of the virtual orbitals, since the CNDO calculations tend to give negative virtual orbital energies, although the results by the ab initio calculations are positive: J. M. Schulman

and J. W. Moskowitz, *J. Chem. Phys.*, **47**, 3491 (1967). In the present CNDO calculation, the lowest unoccupied molecular orbital, $e_{2u}(\pi^*)$, of benzene itself is calculated at -0.50 eV.
(22) A. D. Buckingham and P. J. Stephens, *Annu. Rev. Phys. Chem.*, **17**, 399 (1966).
(23) P. O. Löwdin, *J. Chem. Phys.*, **18**, 365 (1950).
(24) J. C. Slater, *Phys. Rev.*, **36**, 57 (1930).
(25) A. Imamura, T. Hirano, C. Nagata, and T. Tsuruta, *Bull. Chem. Soc. Jpn.*, **45**, 396 (1972).
(26) M. Suzuki, Y. Nihei, and H. Kamada, *Bull. Chem. Soc. Jpn.*, **42**, 323 (1969).
(27) L. Seamans and A. Moscowitz, *J. Chem. Phys.*, **56**, 1099 (1972).
(28) D. J. Caldwell and H. Eyring, *J. Chem. Phys.*, **58**, 1149 (1973).
(29) (a) P. N. Schatz and A. J. McCaffery, *Q. Rev., Chem. Soc.*, **23**, 552 (1969); (b) P. J. Stephens, *Annu. Rev. Phys. Chem.*, **25**, 201 (1974).
(30) (a) S. Nagakura, M. Kojima, and Y. Maruyama, *J. Mol. Spectrosc.*, **13**, 174 (1964); (b) K. Kimura and S. Nagakura, *Mol. Phys.*, **8**, 117 (1965); (c) *Theor. Chim. Acta*, **3**, 164 (1965).
(31) In ref 30b, the expression "strong substituents" was used in such a sense that the absorption spectra of the benzenes with the strong substituents are much different from that of benzene itself.
(32) J. Del Bene and H. H. Jaffé, *J. Chem. Phys.*, **49**, 1221 (1968).

Excitation Functions of Slow Proton Transfer Reactions Involving Negative Ions

## C. Lifshitz,[†] R. L. C. Wu, and T. O. Tiernan*

Contribution from The Brehm Laboratory and Department of Chemistry, Wright State University, Dayton, Ohio 45435. Received September 1, 1977

Abstract: Excitation functions were determined for a series of slow proton and deuteron transfer reactions involving negative ions using a tandem mass spectrometer. Some of the reactions observed, for example, $ND_2^- + D_2 \rightarrow D^- + ND_3$, exhibit translational energy thresholds, even though they are exothermic. Other reactions, such as $CH_3COCH_2^- + CD_3COCD_3 \rightarrow CH_3COCH_2D + CD_3COCD_2^-$, exhibit a complex functional dependence of the cross section upon relative translational energy, which in turn is quite sensitive to the internal energy of the neutral reactant. Rate coefficients determined for these negative ion reactions in the present investigation are compared with analogous data previously reported for thermal energy reactants. The translational energy thresholds observed for several of the reactions are consistent with the existence of a potential energy barrier in the reaction coordinate between the reactants and products. It is demonstrated that the deconvoluted excitation function for the ND_2^-/D_2 reaction is of the form $\sigma \propto (E_{rel} - E_0)^{1/2}/E_{rel}$, as required by theory, and that the translational energy threshold corresponds to the Arrhenius activation energy for this process.

Among the many gas-phase ion–neutral reactions which have been studied, proton transfer processes have perhaps been the subject of greatest interest recently, owing largely to their important role in solution chemistry.[1,2] Much of the recent research has been concerned with proton transfer to negative ions, and has focused on the determination of rate coefficients for thermal energy reactions, and the application of such data in constructing gas-phase acidity and basicity scales.[3] While the rates for many of these reactions are typical of those usually observed for exothermic or thermoneutral reactions, several interesting exceptions have been observed. In particular, certain exothermic proton transfer reactions of amide ions[4,5] and of larger delocalized negative ions[6] have been found to be remarkably slow. These observations prompted some tentative conclusions with respect to the dynamics of slow proton transfer reactions of negative ions.[5,6] Such conclusions, based solely on the magnitude of rate coefficients measured at a single temperature, cannot of course provide a detailed picture of the reaction dynamics, since a low rate coefficient for a particular proton transfer reaction of this type could be explained by either an activation energy barrier (as has been suggested for the amide ion reactions[5]) or by a low entropy factor (as suggested for the delocalized negative ion reac-

tions[6]). Obviously, in some cases, both factors might be operative.

Owing to the limitations of rate data which were just discussed, increasing interest has developed in the determination of translational energy dependences of reactive scattering cross sections (so-called "excitation functions") as a probe of reaction dynamics.[7,8] Such data can provide considerable information with respect to energy barriers for reactions of interest. This is well illustrated by investigations of the three closely related processes,

$$D^+ + H_2 \rightarrow HD + H^+ \qquad (1)$$

$$D + H_2 \rightarrow HD + H \qquad (2)$$

$$D^- + H_2 \rightarrow HD + H^- \qquad (3)$$
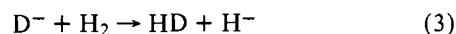
which have been discussed by Henchman et al.[9,10] All three of these are nominally thermoneutral reactions. However, the excitation functions for reactions 2 and 3, which are quite similar, both exhibit translational energy thresholds, whereas reaction 1 exhibits no threshold, and its cross section decreases monotonically with increasing energy.[9-11] These results are consistent with the calculated potential surfaces on which these reactions proceed, since the surfaces relevant to reactions 2 and 3 show energy barriers between the reactants and products,[12,13] while the surface relevant to reaction 1 contains a deep basin

† On sabbatical leave from The Hebrew University of Jerusalem, 1976–1977.

in the reaction coordinate between the reactant and product species.[14]

In the present study, we have determined excitation functions for several thermoneutral and exothermic proton transfer reactions of negative ions, for which thermal rate data have been previously reported. It was expected that these measurements would provide additional insight into the dynamics of these gas-phase processes.

Experimental Section

Materials. The chemicals utilized in this work were obtained from commercial sources, and were used without further purification. Acetone-d_6 (99.5% D) was obtained from Stohler Isotope Chemicals while HD (98% D) and ND_3 (99% D) were supplied by Merck Sharp and Dohme of Canada, Ltd.

Instrumentation. An in-line tandem mass spectrometer, previously described,[15] was utilized for these studies. Briefly, it is a beam-collision chamber apparatus which provides mass analysis of the product ions. The collection stage is fixed at 0° (LAB) scattering angle. The projectile ion is formed in the electron impact ion source of the first stage mass spectrometer, which produces a mass and energy resolved beam. This beam is then decelerated in a retarding lens and impacted upon the target gas in the field-free collision chamber maintained at a constant temperature and pressure. The energy spread of the projectile ion beam entering the collision cell is ±0.3 eV (LAB) over the ion energy range 0.3 to about 180 eV (LAB). Collision chamber temperatures and pressures employed range from 30 to 170 °C and from 5×10^{-3} to 20×10^{-3} Torr, respectively. Product ions are mass analyzed in the second stage mass spectrometer. Pulse counting techniques are used to measure the product ion current.

Preparation of Reactant Ions. Reactant ions are produced by dissociative electron attachment using appropriate source molecules, as described previously,[15] or by ion–molecule reactions occurring in the first-stage ion source. D^- and ND_2^- ions were formed by dissociative electron capture to ND_3. Typical currents of these ions obtained in the tandem mass spectrometer were 1.5×10^{-11} and 1.5×10^{-10} A, respectively. Organic negative ions were produced by proton transfer from selected molecules to O^-. For example, a mixture of N_2O (which forms O^- by dissociative electron capture) and acetone was employed to produce $CH_3C(O^-)=CH_2$ (m/e 57) via the well-known proton transfer reaction from acetone to O^-.[16]

Collection Efficiency. Several experiments were conducted in an effort to assess the degree to which the collection efficiency of the product ions varies with incident ion energy in the reactions studied here. Such variations could be the result of increased momentum transfer at higher velocities and could seriously affect the shapes of the measured excitation functions. The technique used by us to estimate the importance of such effects involves the measurement of "ion beam profiles", and has been described previously.[17,18] The angular divergence of the product beam as it exits from the collision chamber is estimated by applying a lateral field across two split focusing electrodes immediately following the chamber. The product ion beam can thus be swept across the collector slit and an angular profile obtained. Measurements of this type indicated that there is very little variation in the degree of forward scattering of the product H^- ion of reaction 3 as the incident D^- ion energy is varied. It thus appears that even if a mechanism such as "spectator stripping"[19] sets in as the incident ion energy is increased, this does not affect the product ion, which in this case presumably serves as the "spectator", to which very little momentum is transferred (the reaction being H^+ stripping). We believe therefore that, although the second stage analyzer of the in-line tandem collects from only a limited angle in the forward scattered product ion beam, the fraction of product ions collected for the reactions studied here is relatively independent of incident ion energy. Thus, the measured excitation functions for negative ion proton transfer reactions reported in the present study should not be seriously distorted by collection efficiency variations.

Data Treatment. The product (secondary) ion intensity $I_s(E_{io})$ is converted to an observed apparent cross section, using the relation[18,20]

$$\sigma_{app}^{obsd}(E_{io}) = C[I_s(E_{io})/P_t]/I_p(E_{io}) \qquad (4)$$

where $I_p(E_{io})$ is the primary ion intensity, E_{io} is the nominal reactant ion energy in the laboratory frame, P_t is the target gas pressure, and

C is a conversion factor. C is determined at $E_{io} = 0.3$ eV using the previously reported cross section of 63 Å^2 and the product ion intensity observed in the present study for the charge transfer reaction $O^-(NO_2,O)NO_2^-$.[18] Rate coefficients reported in this study were derived from the experimentally measured cross sections, σ_{app}^{obsd}, using the relation $k = \sigma_{app}^{obsd} \bar{v}$, where $\bar{v}$ is the average incident ion velocity at the laboratory energy utilized.

The absolute cross section $\sigma(E_{rel})$ and its dependence upon the true relative energy of the ionic and neutral reactants can in principle be deduced from the experimentally observed dependence of σ_{app}^{obsd} (E_{io}) on the nominal ion laboratory energy E_{io}. The experimentally obtained excitation function differs from the absolute function owing to two factors: (1) the translational energy distribution of the incident ion beam, and (2) the thermal (Doppler) velocity distribution of the neutral target. The second factor (which results in Doppler broadening) is of particular importance for the case in which heavy projectile ions are impacted on light targets. The manner in which the absolute excitation functions are deduced from experimentally observed functions has been described in detail previously.[15,21]

Results and Discussion

1. D^- Reactions. Table I lists the rate coefficients determined in the present study for several proton transfer reactions to D^-, at a reactant ion translational energy of 0.3 eV (LAB). No previously reported data with which these values can be directly compared is available. Paulson[22] has reported a value of $k = 15 \times 10^{-10}$ cm^3/molecule·s at $E_{lab} = 0.6$ eV for the D^-/D_2O proton transfer reaction, an isotopic variant of the D^-/H_2O reaction studied here. The reactions of D^- with H_2O, HCl, C_2H_2, H_2S, and CH_3OH are observed to be very fast (on the order of gas kinetic collision rates). These reactions, as shown in Table I, are all exothermic; that is, the neutral molecules are stronger acids in the gas phase than is HD.[24,25,39] Betowski et al.[26] determined rate coefficients for a series of proton transfer reactions involving both positive and negative ions, and their results indicate that the experimental rate coefficients are generally larger than the Langevin rates by a factor of 3 or 4, in the case of those reactions which are highly exothermic (>30 kcal/mol). This is not surprising since these reactions involved polar molecules, and the permanent dipole moments of the latter lead to increased reactivity. On the other hand, several proton transfer reactions from polar molecules to negative ions which are only slightly exothermic (including the H^-/H_2O reaction) were found to have experimental rate coefficients which exceed the Langevin rate by a smaller factor. Betowski et al.[26] noted that this reduced probability for slightly exothermic proton transfer reactions might be a consequence of the reaction mechanism, or alternatively, could result from a small activation energy barrier. The excitation function determined in the present study for the analogous D^-/H_2O reaction (and the other fast negative ion proton transfer processes mentioned above) give no indications of energy thresholds for these processes, and therefore any activation barriers for these processes must be smaller than the lower limit of the ion translational energy attainable in our apparatus (~0.3 eV, LAB).

In the studies discussed above, Betowski et al.[26] found that the experimental rate coefficients for highly exothermic proton transfer reactions involving polar molecules were in better agreement with the values calculated using the ADO theory than with the Langevin rates. As can be seen from the data in Table I, this does not seem to be the case for the negative-ion polar molecule reactions studied here.

Rate coefficients for the reactions of D^- with H_2, NH_3, and ND_3 are also shown in Table I, and are seen to be rather small in comparison with those for the reactions just discussed. In addition, the excitation functions for the reactions of D^- with H_2, NH_3, and ND_3 were found to exhibit translational energy thresholds, which are indicative of activation barriers for these processes. Figure 1 shows the excitation function measured for

Table I. Rate Coefficients for Various Proton Transfer Reactions to D^- and NH_2^-

XH	k_{exp}, 10^{-10} cm^3/molecule·s^{a,b}	$k_L{}^c$ 10^{-10} cm^3/molecule·s	$k_{ADO}{}^d$	k_{exp}/k_{ADO}	$-\Delta H_{298K}^{\circ}$,^{e} kcal/mol
	1. D^- Reactions; $D^- + XH \rightarrow X^- + HD$				
CH$_3$OH	19	30.7	39.1	0.49	20
H$_2$O	22	21.0	32.9	0.67	10
HCl	17	27.6	32.2	0.53	67
C$_2$H$_2$	19	31.4	31.4	0.60	~30
H$_2$S	26	33.1	36.6	0.71	50
CCl$_3$H	0.67	48.0	50.8	0.013	f
H$_2$	0.3	20.8	20.8	0.014	0
NH$_3$	0.2	26.3	34.8	0.0057	−2.6
ND$_3$	0.06$_5$	26.1	34.6	0.0019	−2.9
	2. NH_2^- and ND_2^- Reactions				
$NH_2^- + H_2 \rightarrow H^- + NH_3$	0.18	15.6	15.6	0.012	3.2
$NH_2^- + D_2 \rightarrow D^- + NH_2D^i$	0.10	11.5	11.5	0.0087	~3.0
$NH_2^- + HD \rightarrow D^- + NH_3$	0.17	6.5^g	6.5	0.026	2.6
$NH_2^- + HD \rightarrow H^- + NH_2D$	0.17	6.5^g	6.5	0.026	~3.0
$ND_2^- + D_2 \rightarrow D^- + ND_3$	0.09	11.4	11.4	0.0079	2.9

^{a} Measured with reactant ions of 0.3 eV laboratory energy and at a collision chamber temperature of 300 K. ^{b} Rate coefficients were determined relative to the rate $k = 1.2 \times 10^{-9}$ cm^3/molecule·s for the reaction $O^- + NO_2 \rightarrow NO_2^- + O$. ^{c} Langevin theory; G. Gioumousis and D. P. Stevenson, *J. Chem. Phys.*, **29**, 294 (1958). ^{d} Average dipole orientation theory; M. T. Bowers and T. Su in ref 1, p 163. Calculated for an effective temperature T such that the center of mass energy $E_{CM} = \frac{3}{2} kT$. ^{e} Calculated from available heats of formation, electron affinities, and proton affinities; H. M. Rosenstock, K. Draxl, B. W. Steiner, and J. T. Herron, *J. Phys. Chem. Ref. Data, Suppl. 1*, **6** (1977); J. L. Beauchamp in ref 1, p 413; K. Tanaka, G. I. Mackay, J. D. Payzant, and D. K. Bohme, *Can. J. Chem.*, **54**, 1643 (1976); S. A. Sullivan and J. L. Beauchamp, *J. Am. Chem. Soc.*, **98**, 1160 (1976). ^{f} Exothermicity uncertain. ^{g} $k_{Langevin}$ divided by statistical factor of 2.
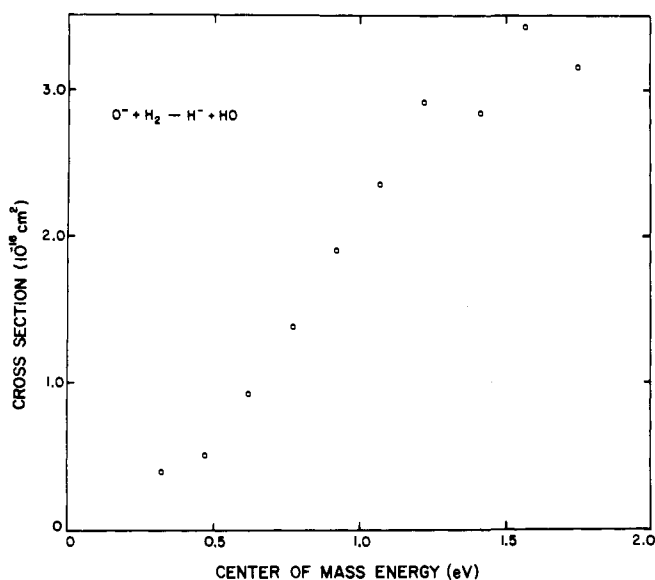

Figure 1. Excitation function for the reaction $D^-(H_2,HD)H^-$; the reaction cross section σ_{app}^{obsd} (see text) is plotted as a function of nominal ion energy (CM).

reaction 3 (not corrected for ion translational energy spread and Doppler broadening). These results are in general agreement with Paulson's data[9-11] and the expectations from theory,[13] which were discussed earlier. The rate coefficients for the D^-/NH_3 and D^-/ND_3 reactions (Table I) are somewhat larger than that determined by Bohme et al.[4] for the analogous H^-/NH_3 reaction ($k = 0.009 \times 10^{-10}$ cm^3/molecule·s). Because the first stage of the tandem mass spectrometer in the present configuration does not transmit H^- ions, we cannot directly observe the latter reaction. In any case, the rate coefficients determined here at an incident ion energy of ~0.3 eV are not directly comparable with those measured at thermal energies by Bohme et al.[4] The energy dependence of the cross section for the D^-/NH_3 proton transfer reaction is rather flat over the entire energy range examined (~0.1–2.4 eV, in the

center of mass system). This behavior is quite similar to that which we have previously observed in the case of D^-/SF_6 electron transfer reaction.[27] In both of these cases, a light incident ion is impacted on a heavy target molecule, and the experimental energy resolution in the laboratory system is approximately the same as that in the center of mass system. The resolution attainable (±0.3 eV) is of the same order of magnitude as the translational energy threshold for the D^-/NH_3 reaction, and it is thus rather difficult to obtain an accurate value for this threshold. The difference in the rate coefficients for the D^-/NH_3 and D^-/ND_3 reactions which are listed in Table I is presumably indicative of kinetic isotope effects.

2. NH_2^- and ND_2^- Reactions. Rate coefficients for amide ion reactions with H_2, HD, and D_2 are also presented in Table I. As for the D^- reactions with ammonia, interesting kinetic isotope effects are observed. Both the forward and reverse steps of the reaction

$$NH_2^- + H_2 \rightleftarrows H^- + NH_3 \qquad (5)$$
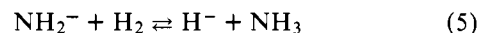
were studied in considerable detail by Bohme and co-workers.[3a,4,5,28] Their results indicate that H_2 is a stronger acid in the gas phase than is NH_3. Bohme et al.[4] reported a rate coefficient of 0.23×10^{-10} cm^3/molecule·s at 298 K for the forward step of reaction 5, which may be compared with our value of 0.18×10^{-10} cm^3/molecule·s, determined at 0.3 eV (Table I). The currently accepted value for the equilibrium constant of reaction 5 is $K_{eq5} = 27 \pm 9$ at 298 K.[4] This value can be used in conjunction with the computed ΔS° for reaction 5 to calculate the difference in the proton affinities of H^- and NH_2^-. The resulting difference is $PA(H^-) - PA(NH_2^-) = -3.2$ kcal/mol. In the present study, we have also observed two isotopic variants of reaction 5, namely,

$$NH_2^- + HD \rightleftarrows D^- + NH_3 \qquad (6)$$

$$ND_2^- + D_2 \rightleftarrows D^- + ND_3 \qquad (7)$$
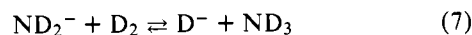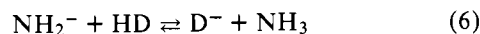
The equilibrium constants of reactions 6 and 7 have not yet been determined experimentally. They can be derived, however, by the usual thermodynamic relations, for example for

reaction 6, eq 8–11.

$$\Delta H°_{298} - T\Delta S°_{298} = \Delta G°_{298} = -RT \ln K_{eq} \qquad (8)$$

$$\Delta H°_{298} = \Delta H°_0 + \int_0^{298} \Delta C_p dT \qquad (9)$$

$$\Delta H°_0 = EA(NH_2) - EA(D) + D°_0(H\text{-}D) - D°_0(NH_2\text{-}H) \qquad (10)$$

$$\Delta S°_{298} = S°_{298}(D^-) + S°_{298}(NH_3) - S°_{298}(NH_2^-) - S_{298}(HD) \qquad (11)$$

Using the appropriate bond dissociation energies, electron affinities, and standard entropies[29] for the species involved in these reactions, one obtains the equilibrium constants $K_{eq\ 6}$ = 0.82 and $K_{eq\ 7}$ = 1.8 at 298 K. (The calcualted proton affinity of D^-, 399.8 kcal/mol, is 0.6 kcal/mol higher than that for H^-.) The value used for the bond dissociation energy $D°_0(NH_2\text{-}H)$ here is taken from the equilibrium study of reaction 5 by Bohme et al.[4] There are two alternative thermochemical values,[4] one higher and one lower than the value obtained from the equilibrium study. Obviously, if one of these alternative values were used in calculating $K_{eq\ 6}$ and $K_{eq\ 7}$ the magnitudes of these equilibrium constants would be different, but of course the value of $K_{eq\ 5}$ cited above would also change, so that the isotope effects on the equilibrium constants would be essentially the same. The computed equilibrium constants may be compared with the ratios of the rate coefficients for the forward and reverse steps of reactions 6 and 7. Using the data shown in Table I, for reaction 6, k_f/k_r = 0.85 and for reaction 7, k_f/k_r = 1.4. In spite of the fact that the reactant ions in the present case are not translationally thermal, the agreement between the calculated equilibrium constants and the ratios, k_f/k_r, is surprisingly good.

As previously noted, reaction 3, and both the forward and reverse steps of reaction 5 and its various deuterated analogues, are relatively slow reactions. Translational energy thresholds were observed for both the forward and reverse steps of the ammonia–hydrogen reactions. The excitation function for the forward step of reaction 7 is shown in Figure 2. This reaction step is exothermic by 2.85 kcal/mol. Yet the excitation function is obviously typical of that observed for reactions which are endoergic or which have an activation barrier. Because of the large ratio of the projectile ion mass to that of the target molecule, the Doppler broadening effect is severe for this reaction. The Doppler width (Δ), which is the half-width of the probability distribution at $1/e$ of the maximum height, is given by the expression[15]

$$\Delta = 2(mE_{io}kT/M)^{1/2} \qquad (12)$$

where m and M are the masses of the ion and neutral, respectively, E_{io} is the nominal reactant ion energy (LAB), T is the collision chamber temperature, and k is the Boltzmann constant. For E_{io} = 2 eV and T = 443 K, Δ = 1.17 eV for the ND_2^-/D_2 reactant pair. The experimental excitation function must be deconvoluted to correct for the Doppler broadening and the ion translational energy distribution, as noted earlier. Since neither the energy threshold for reaction 7 nor the postthreshold energy dependence of the cross section is known, trial "absolute" excitation functions were tested until a best fit was achieved between the calculated convoluted curve[15,21] and the experimental data of Figure 2. The excitation function expected from theory[30] for an endoergic ion–molecule reaction has the functional form

$$\sigma(E_{rel}) = \pi Y(E_{rel})/k^2 \qquad (13)$$

where the "yield function" is given by

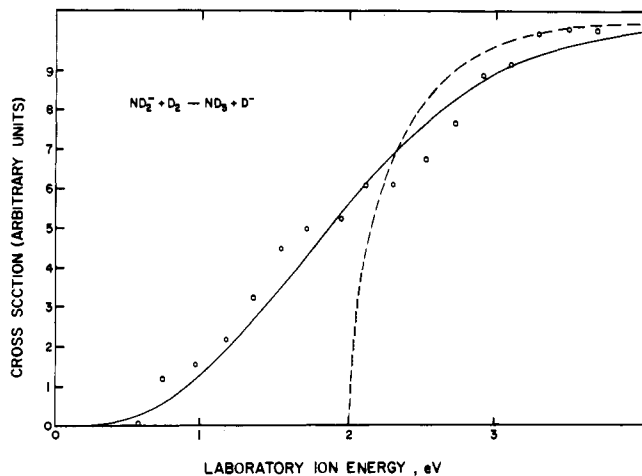$$Y(E_{rel}) = (S\mu/\hbar^2)C_s^{2/S}[2(E_{rel} - E_0)/(S - 2)]^{1-2/S} \qquad (14)$$

Figure 2. Excitation function for the reaction $ND_2^-(D_2,ND_3)D^-$; points are experimental data for σ_{app}^{obsd} (in arbitrary units) as a function of the nominal ion energy (lab). The experimental cross section at the maximum is ~1.8 × 10^{-16} cm^2 at a nominal ion energy (CM) of 0.6 eV, and drops at higher energies (not shown). The smooth curve is the computer fit to the data, obtained by convoluting the dashed curve, representing the absolute excitation function in the laboratory frame, with the ion translational energy distribution and the Doppler broadening distribution function (see ref 21).

and

$$k^2 = (2\mu/\hbar^2)E_{rel} \qquad (15)$$

where E_{rel} is the relative translational energy (CM), E_0 is the translational energy threshold (CM), S = 4, and $C_s = \alpha e^2/2$ for an ion-induced dipole interaction, α is the polarizability of the neutral, e is the electronic charge, and $\hbar = h/2\pi$, where h is Planck's constant and μ is the reduced mass of the ion-neutral pair. Inserting eq 14 and 15 into eq 13, one obtains

$$\sigma(E_{rel}) = 2\pi(\alpha e^2/2)^{1/2} \frac{(E_{rel} - E_0)^{1/2}}{E_{rel}} \qquad (16)$$

Employing this functional form, and treating E_0 as a parameter, the best fit of the computer calculated curve to the experimental data (see Figure 2) corresponds to an energy threshold of E_0 = 2 eV (LAB) or E_0 = 0.36 (CM) = 8.4 kcal/mol. We can now consider the relationship between this translational energy threshold, E_0, and the Arrhenius activation energy, E_a, for the reaction. The temperature-dependent rate coefficient, $k(T)$,[30-32] is related to the cross section by the expression

$$k(T) = (2/kT)^{3/2}(1/\pi\mu)^{1/2}$$
$$\times \int_0^\infty e^{-E_{rel}/kT}\sigma(E_{rel})E_{rel} dE_{rel} \qquad (17)$$

Inserting eq 16 into eq 17, the rate coefficient is then given by

$$k(T) = 2\pi e(\alpha/\mu)^{1/2}e^{-E_0/kT} \qquad (18)$$

or, in other terms,

$$k(T) = k_{coll}e^{-E_0/kT} \qquad (19)$$

where k_{coll} is the Langevin collision rate coefficient. The Arrhenius activation energy is given as usual by[30]

$$E_a = RT^2 d \ln k(T)/dT \qquad (20)$$

so it is apparent that $E_a = E_0$. In their treatment of similar proton transfer reactions, Mackay, Hemsworth, and Bohme[5] have tentatively assumed that

$$k_{exptl} = k_{coll}e^{-E_a/kT} \qquad (21)$$

Table II. Rate Coefficients for Proton Transfer Reactions to Organic Negative Ions

Reaction	k, 10^{-10} cm^3/molecule·s	
	Present[a,b]	Values reported previously
$CH_3O^- + CD_3OH \rightarrow CD_3O^- + CH_3OH$	6.76	
$CH_3O^- + C_6H_5CH_3 \rightarrow C_7H_7^- + CH_3OH$	6.58	2.0[c]
$CH_2=CHCH_2^- + CH_3OH \rightarrow CH_3O^- + C_3H_6$	10.9	2.5[c]
$CH_2=CHCH_2^- + C_6H_5CH_3 \rightarrow C_7H_7^- + C_3H_6$	≤0.005	0.75;[c] ~0.1[d]
$CH_2=CHCH_2^- + CD_2=CDCD_3 \rightarrow C_3D_5^- + C_3H_5D$	0.0018	
$CH_3C(O^-)=CH_2 + CD_3C(=O)CD_3 \rightarrow CD_3C(O^-)=CD_2 + CH_3COCH_2D$	0.032[e]	0.032[g]
	0.014[f]	
$CD_3C(O^-)=CD_2 + CH_3C(=O)CH_2CH_3 \rightarrow CH_3C(O^-)=CHCH_3 + CD_3COCD_2H$	0.1[e]	0.064[g]
	0.032[f]	

[a] Measured with reactant ions of ~0.3 eV laboratory energy. [b] Rate coefficients were determined relative to the rate $k = 1.2 \times 10^{-9}$ cm^3/molecule·s for the reaction $O^- + NO_2 \rightarrow NO_2^- + O$. [c] Measured by the ICR method at 300 K (ref 23). [d] Measured by the flowing afterglow method at 300 K (ref 3a). [e] Collision chamber temperature 300 K. [f] Collision chamber temperature 440 K. [g] Measured by the ICR method at 300 K (ref 6).
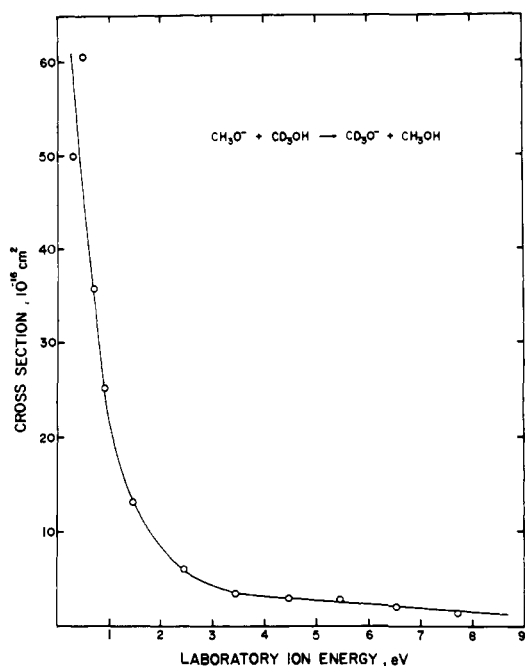
Figure 3. Excitation function for the reaction CH$_3$O$^-$(CD$_3$-OH,CH$_3$OH)CD$_3$O$^-$.

Figure 4. Excitation function for the reaction CH$_2$=CH-CH$_2^-$(CH$_3$OH,C$_3$H$_6$)CH$_3$O$^-$.

From the above discussion, it is seen that this is equivalent to our assumed excitation function, with $E_a = E_0$. Using eq 21 Mackay et al.[5] computed for the forward step of reaction 5 an activation energy $E_a = 2.5$ kcal/mol. This is somewhat lower than the value of 8.4 kcal/mol obtained in the present study for the forward step of reaction 7, the difference being well outside the experimental error limits of the two measurements. Apparently, this difference reflects a true isotope effect, although the activation energy value derived here must be considered as an upper limit. It was observed that other trial excitation functions, which rise less sharply at threshold than does the function represented by eq 16, could also be fit to the experimental data (upon convolution with the energy distribution), provided that the threshold parameter, E_0, was less than 2 eV (in the laboratory system). That is to say, from our results, we can calculate only that $E_0 \leq 8.4$ kcal/mol.

Threshold behavior similar to that described above was also observed for the forward step of reaction 5 and the magnitude of the barrier seems to be slightly lower than that estimated for the ND$_2^-$/D$_2$ reaction.

3. Organic Negative Ion Reactions. The rate coefficients measured in the present study for a number of organic negative ion proton transfer reactions are shown in Table II. The rate
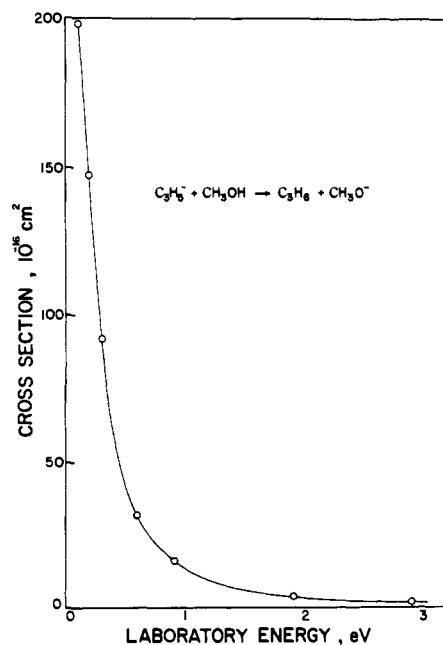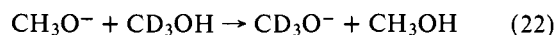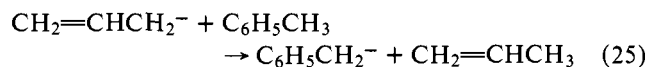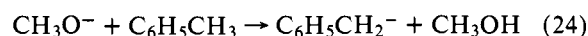
coefficient for the reaction

$$CH_3O^- + CD_3OH \rightarrow CD_3O^- + CH_3OH \qquad (22)$$

is approximately half the collision rate constant,[6] which suggests that this reaction involves the formation of a hydrogen-bonded intermediate, which can decompose to give either the observed products or the original reactants, with equal probabilities. Such organic ion–molecule reactions involving polyatomic species are now generally considered to proceed at low energies via intermediate complexes which decompose in various ways depending upon energy content.[25,33] The excitation function for reaction 22, shown in Figure 3, is typical for a reaction having no activation barrier. Reactions 23, 24, and 25 were also observed previously[23] under thermal energy conditions. In these earlier studies, reactions 23 and 24 were found to be fast, while reaction 25 was shown to be slow.
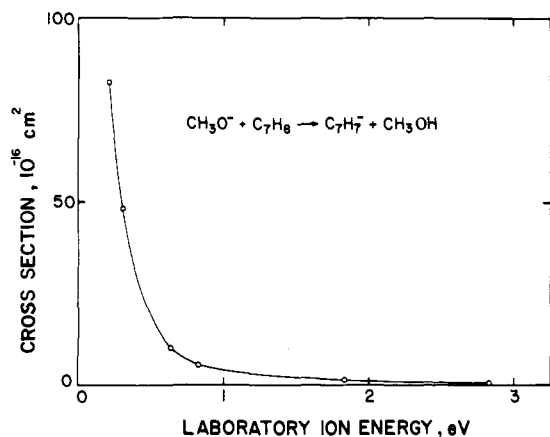
$$CH_2=CHCH_2^- + CH_3OH \rightarrow CH_3O^- + CH_3CH=CH_2 \qquad (23)$$

$$CH_3O^- + C_6H_5CH_3 \rightarrow C_6H_5CH_2^- + CH_3OH \qquad (24)$$

$$CH_2=CHCH_2^- + C_6H_5CH_3$$
$$\rightarrow C_6H_5CH_2^- + CH_2=CHCH_3 \qquad (25)$$
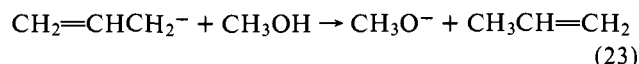
Figure 5. Excitation function for the reaction CH_3O^--$(C_6H_5CH_3,CH_3OH)C_7H_7^-$.
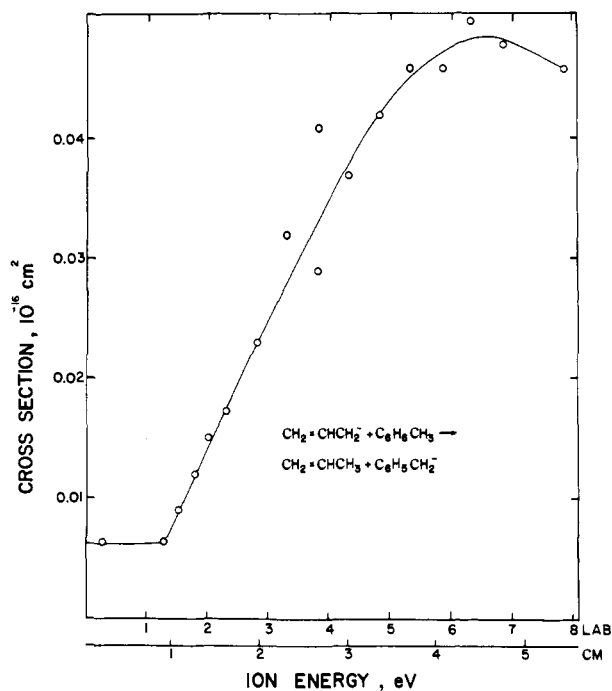
Figure 6. Excitation function for the reaction $C_3H_5^-(C_7H_8,C_3H_6)C_7H_7^-$. Note that the plots have not been corrected for Doppler broadening.

Figure 7. Excitation function for the reaction $(C_3D_6,$ $C_3H_5D)C_3D_5^-$. The data have not been corrected for Doppler broadening.
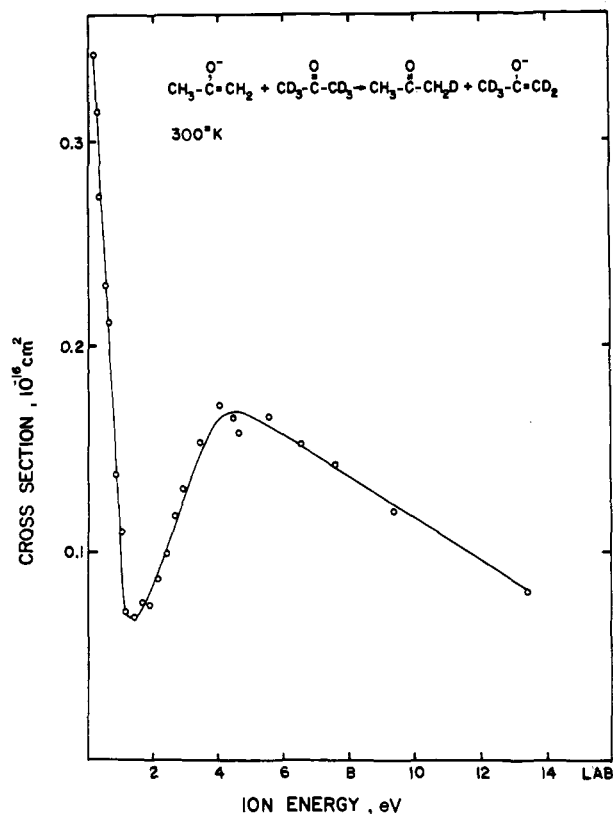
Figure 8. Excitation function for the reaction $CH_3COCH_2^-$-$(CD_3COCD_3,CH_3COCH_2D)CD_3COCD_2^-$. Collision chamber temperature is 300 K.

These observations lead to the conclusion that in a mixture of these components, the presence of methanol catalyzes the conversion of allyl anion to benzyl anion. Figures 4–6 show the excitation functions measured in the present study for reactions 23, 24, and 25. As shown, these are uncorrected for the Doppler broadening effect. As expected, the reactions 23 and 24 do not exhibit translational energy thresholds. However, although reaction 25 is exothermic, the excitation function for this process clearly indicates a translational energy threshold. Similar threshold behavior is observed (Figure 7) for the nominally thermoneutral reaction

$$CH_2\!\!=\!\!CHCH_2^- + CD_2\!\!=\!\!CDCD_3 \rightarrow C_3D_5^- + C_3H_5D$$

$$(26)$$

These results indicate the existence of energy or activation barriers in the potential surfaces of some proton transfer reactions to delocalized negative ions. The magnitude of the thresholds is indicative of activation barriers on the order of $\simeq 10$ kcal/mol. There is surprising disagreement between the rate coefficient measured in the present study for reaction 25
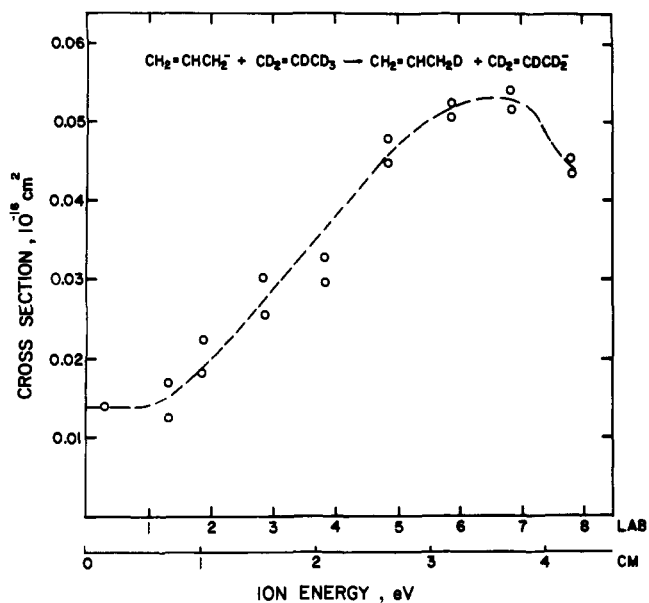
and those previously reported[3a,23] (Table II). We believe, however, that the low rate coefficient which we obtained is consistent with the observation of a high activation barrier. The rate coefficients of reactions 25 and 26 were rather insensitive to the collision chamber temperature (in the range 300–440 K) increasing only slightly at the higher temperature. However, the rate of reaction 25 was observed to be extremely sensitive to the presence of impurities in the collision chamber,
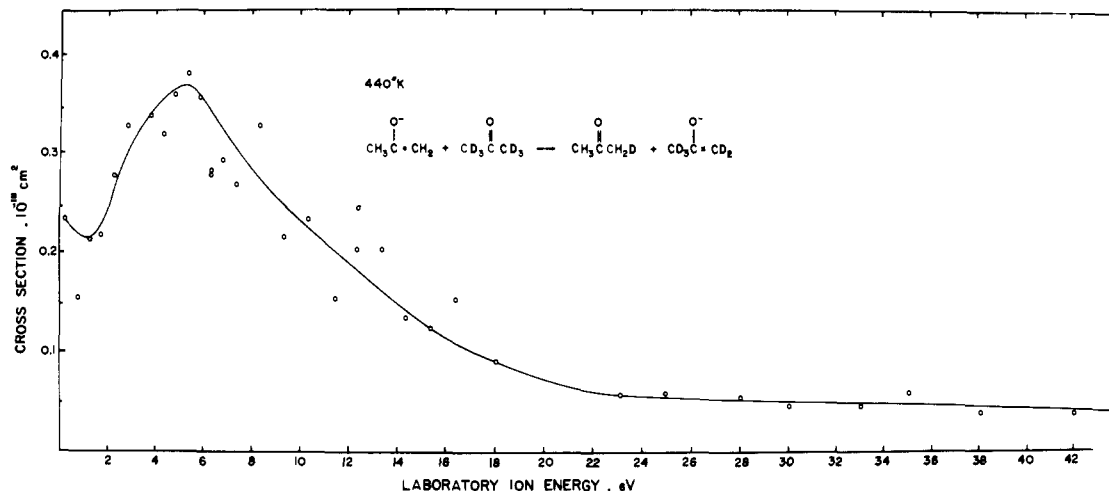
Figure 9. Excitation function for the reaction $CH_3COCH_2^-(CD_3COCD_3,CH_3COCH_2D)CD_3COCD_2^-$. Collision chamber temperature is 440 K.
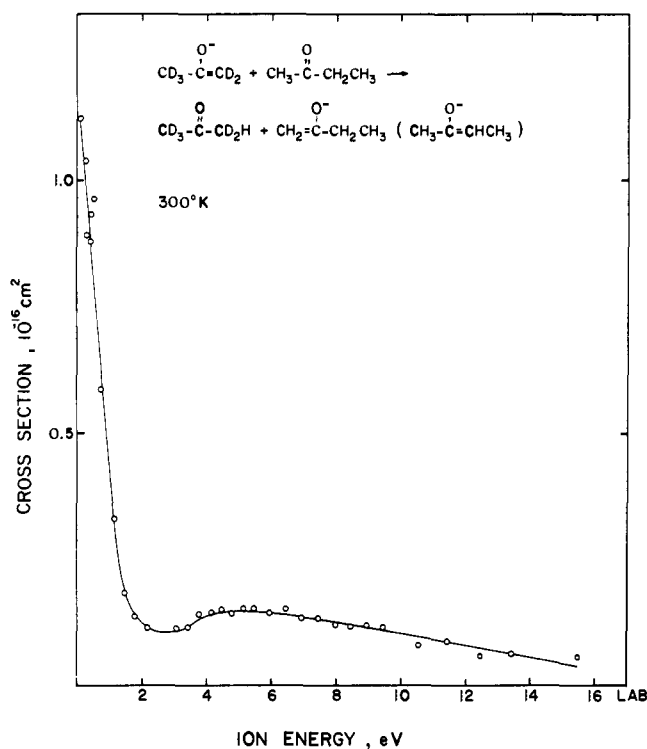
Figure 10. Excitation function for the reaction $CD_3COCD_2^-$ $(CH_3COCH_2CH_3,CD_3COCD_2H)CH_3COCHCH_3^-$. Collision chamber temperature is 300 K.
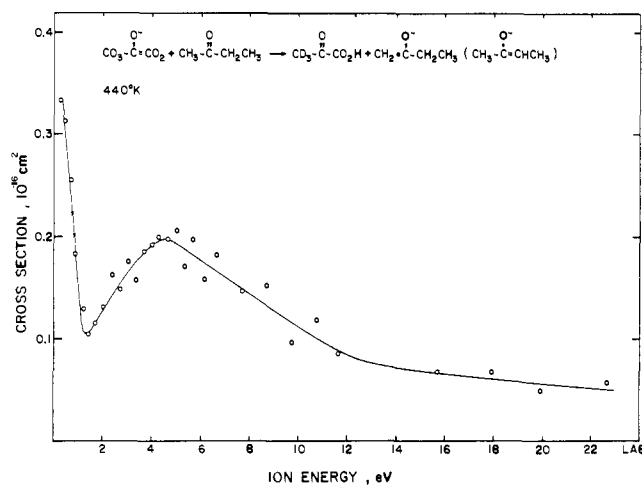
Figure 11. Excitation function for the reaction $CD_3COCD_2^-$ $(CH_3COCH_2CH_3,CD_3COCD_2H)CH_3COCHCH_3^-$. Collision chamber temperature is 440 K.
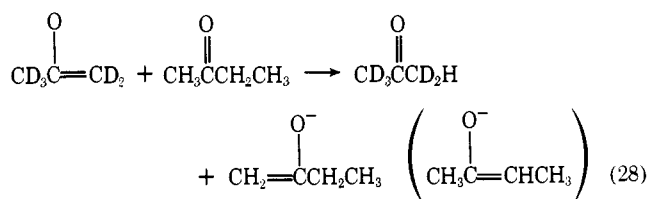
the rate increasing dramatically in the presence of even trace quantities of methanol, in agreement with the ICR data.[23] Thus, realistically, the rate coefficient reported here probably represents at best an upper limit. It seems probable that the values previously reported[3a,23] are also upper limits, since the presence of trace impurities in the afterglow and ICR experiments would have a similarly adverse effect.

Of special interest are the reactions of delocalized enolate anions with aliphatic ketones, such as

$$CH_3\underset{|}{\overset{O^-}{C}}=CH_2 + CD_3\overset{O}{\overset{\|}{C}}CD_3 \longrightarrow CH_3\overset{O}{\overset{\|}{C}}CH_2D + CD_3\underset{|}{\overset{O^-}{C}}=CD_2 \quad (27)$$
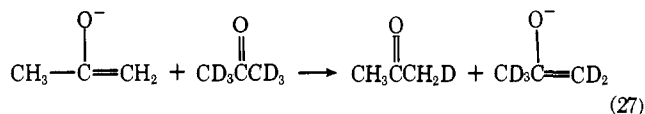
Reaction 27 is nominally thermoneutral, while reaction 28 is slightly exothermic (for formation of either ionic product).[6] The rate coefficients of these reactions were determined in the present study and are compared with previous data in Table II. Excitation functions were also measured for each reaction at both low (300 K) and high (440 K) collision chamber temperatures. These functions are shown in Figures 8–11 and the corresponding rate coefficients for these reactions are plotted as a function of translational energy in Figures 12 and 13. These excitation functions do not exhibit translational energy thresholds. On the contrary, in the low kinetic energy range, the cross section drops with increasing energy in a manner typical of exoergic reactions, having no activation barrier. This result is consistent with the model suggested by Farneth and Brauman,[6] which predicts that there are activation barriers

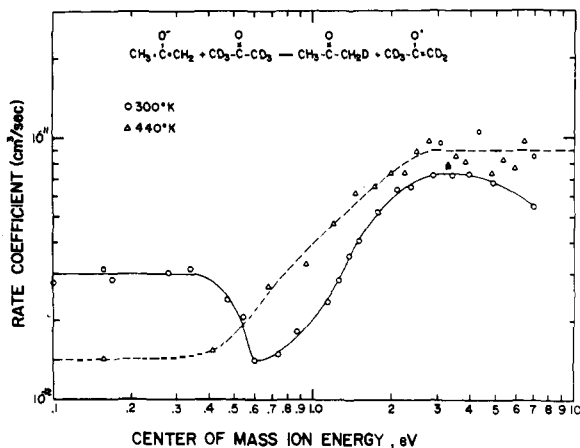$$CD_3\overset{O}{\overset{\|}{C}}=CD_2 + CH_3\overset{O}{\overset{\|}{C}}CH_2CH_3 \longrightarrow CD_3\overset{O}{\overset{\|}{C}}CD_2H$$

$$+ CH_2\underset{|}{\overset{O^-}{=}}CCH_2CH_3 \left(CH_3\underset{|}{\overset{O^-}{C}}=CHCH_3 \right) \quad (28)$$

Figure 12. Rate coefficients for the reaction $CH_3COCH_2^-(CD_3CO-CD_3,CH_3COCH_2D)CD_3COCD_2^-$ as a function of relative translational energy at the two collision chamber temperatures indicated.

Figure 13. Rate coefficients for the reaction $CD_3COCD_2^-$ $(CH_3COCH_2CH_3,CD_3COCD_2H)CH_3COCHCH_3^-$ as a function of relative translational energy at the two collision chamber temperatures indicated.

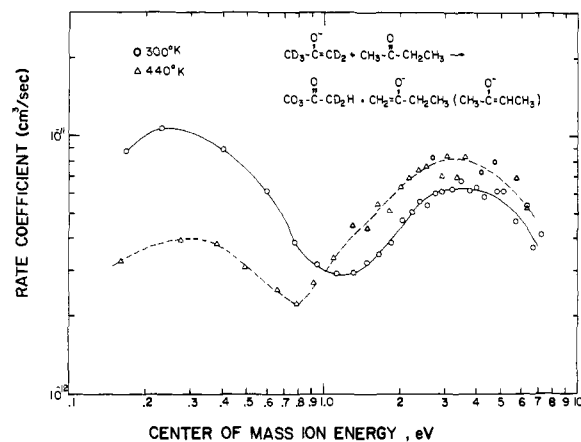in the potential surfaces appropriate to reactions 27 and 28, but that the height of these barriers is *lower* than the potential energies of either the separated reactants or products. This barrier corresponds to the symmetrical transition state for proton transfer, the reaction proceeding via a three-step mechanism involving the formation of a nonsymmetrical intermediate, $[AH---B]^-$, which lies in a potential well with respect to the reactants, $(AH + B^-)$, as well as with respect to the transition state, $(A---H---B)^-$. According to this model,[6] it is the competition between two unimolecular decompositions of the intermediate, the back reaction forming $(AH + B^-)$ via a simple bond cleavage, and the forward rearrangement reaction, producing the symmetrical transition state, which determines the overall bimolecular rate coefficient at thermal energies. This model is well supported by the present results. We observe that the rate coefficient and its variation with translational energy (Table II and Figures 12 and 13) are strongly dependent on the collision chamber temperature. At low translational energies, it is seen that an increase in the collision chamber temperature decreases the overall rate coefficient. A similar effect has been observed in certain hydride ion transfer reactions of large polyatomic positive ions.[34] Increasing the collision chamber temperature results in an increase in the internal energy of the neutral reactant, and in turn, the internal energy of the intermediate, E^*, is increased. The larger internal energy of the intermediate favors the unimolecular channel having a high activation energy and a high entropy factor, that is, the simple bond cleavage, which corresponds to the back reaction yielding the original reactants. An increase in the cross section with increasing translational energy is observed at energies greater than ~ 1.5 eV in the laboratory system. This may reflect a change in the mechanism of the reaction, resulting from the fact that the long-lived intermediate can no longer be formed at the higher interaction energies. It is well known that the mechanism of an ion–neutral reaction can change from one involving formation of a persistent intermediate complex to a direct mechanism as the collision energy is increased.[35] The lifetime of such an intermediate collision complex decreases with increasing internal energy E^*, and in turn the internal energy increases as the relative energy of the reactants is increased. When the interaction energy increases to the point that the intermediate is no longer formed, back reaction to give reactants can no longer compete effectively with the forward reaction, and an increase in the cross section (and of k) with increasing energy is then observed. This rationale is further supported by the fact that the point of onset of the rising portion of the plot of k as a function of ion energy shifts to lower relative energies as the

temperature is increased (Figures 12 and 13). This demonstrates the equivalent role of internal and relative translational energy in reducing the lifetime of the intermediate complex. The second decrease in the cross section at still higher energies (Figures 8–11) is consistent with the behavior of many ion-molecule reactions at higher energies and presumably simply reflects a decrease in the collision cross section.

References and Notes

(1) D. K. Bohme in "Interactions between Ions and Molecules", P. Ausloos, Ed., Plenum Press, New York, N.Y., 1975, p 489.
(2) S. G. Lias and P. Ausloos in "Ion-Molecule Reactions: Their Role in Radiation Chemistry", ERDA/ACS, Washington, D.C., 1975, p 90.
(3) See, for example, (a) D. K. Bohme, E. Lee-Ruff, and L. B. Young, *J. Am. Chem. Soc.*, **94**, 5153 (1972); (b) S. A. Sullivan and J. L. Beauchamp, *ibid.*, **98**, 1160 (1976); (c) T. B. McMahon and P. Kebarle, *ibid.*, **98**, 3399 (1976).
(4) D. K. Bohme, R. S. Hemsworth, and H. W. Rundle, *J. Chem. Phys.*, **59**, 77 (1973).
(5) G. I. Mackay, R. S. Hemsworth, and D. K. Bohme, *Can. J. Chem.*, **54**, 1624 (1976).
(6) W. E. Farneth and J. I. Brauman, *J. Am. Chem. Soc.*, **98**, 7891 (1976).
(7) M. E. Gersh and R. B. Bernstein, *J. Chem. Phys.*, **55**, 4661 (1971); M. E. Gersh and R. B. Bernstein, *ibid.*, **56**, 6131 (1972); H. E. Litvak, A. González Ureña, and R. B. Bernstein, *ibid.*, **61**, 4091 (1974).
(8) See, for example, M. Henchman in "Ion-Molecule Reactions", J. L. Franklin, Ed., Plenum Press, New York, N.Y., 1972, pp 101–245.
(9) J. Dubrin and M. J. Henchman, *MTP Int. Rev. Sci.: Phys. Chem.*, Sect 1, **9** (1972).
(10) M. J. Henchman in ref 1, p 15.
(11) J. F. Paulson, *Bull. Am. Phys. Soc.*, Ser. II, **17**, 401 (1972).
(12) I. Shavitt, R. M. Stevens, F. L. Minn, and M. Karplus, *J. Chem. Phys.*, **48**, 2700 (1968).
(13) C. D. Ritchie and H. F. King, *J. Am. Chem. Soc.*, **90**, 825 (1968).
(14) (a) I. G. Csizmadia, R. E. Karl, J. C. Polanyi, A. C. Roach, and M. A. Robb, *J. Chem. Phys.*, **52**, 6205 (1970); (b) R. K. Preston and J. C. Tully, *ibid.*, **54**, 4297 (1971).
(15) T. O. Tiernan, B. M. Hughes, and C. Lifshitz, *J. Chem. Phys.*, **55**, 5692 (1971).
(16) (a) J. H. Futrell and T. O. Tiernan in "Ion-Molecule Reactions", Vol. 2, J. L. Franklin, Ed., Plenum Press, New York, N.Y., 1972, pp 543–545; (b) A. G. Harrison and K. R. Jennings, *J. Chem. Soc., Faraday Trans. 1*, **72**, 1601 (1976).
(17) T. O. Tiernan and B. M. Hughes, "Product Ion Deflection Measurements as an Indication of the Mechanisms of Low-Energy Ion-Molecule Reactions", 18th Annual Mass Spectrometry Conference (ASTM), San Francisco, Calif., 1970.
(18) T. O. Tiernan in ref 1, pp 353 and 601–604.
(19) A. Henglein, *Adv. Chem. Ser.*, **No. 58**, 63 (1966).
(20) D. G. Hopper, A. C. Wahl, R. L. C. Wu, and T. O. Tiernan, *J. Chem. Phys.*, **65**, 5474 (1976).
(21) C. Lifshitz, R. L. C. Wu, T. O. Tiernan, and D. T. Terwilliger, *J. Chem. Phys.*, **68**, 247 (1978).
(22) J. F. Paulson in "Ion-Molecule Reactions", Vol. 1, J. L. Franklin, Ed., Plenum

Press, New York, N.Y., 1972, p 77.
(23) J. I. Brauman, C. A. Lieder, and M. J. White, *J. Am. Chem. Soc.*, **95**, 927 (1973).
(24) D. Holtz, J. L. Beauchamp, and J. R. Eyler, *J. Am. Chem. Soc.*, **92**, 7045 (1970).
(25) J. L. Beauchamp in ref 1, p 413.
(26) D. Betowski, J. D. Payzant, G. I. Mackay, and D. K. Bohme, *Chem. Phys. Lett.*, **34**, 321 (1975).
(27) C. Lifshitz, T. O. Tiernan, and B. M. Hughes, *J. Chem. Phys.*, **59**, 3182 (1973).
(28) L. B. Young, E. Lee-Ruff, and D. K. Bohme, *Can. J. Chem.*, **49**, 979 (1971).
(29) D^0(HD) and D^0(D$_2$), G. Herzberg, "Molecular Spectra and Molecular Structure", Vol. I, 2nd ed, Van Nostrand, Princeton, N.J.; EA(NH$_2$) and D^0(NH$_2$–H) from ref 4; EA(D), K. E. McCulloh and J. A. Walker, *Chem. Phys. Lett.*, **25**, 439 (1974); S^0(NH$_3$) and S^0(NH$_2^-$) from ref 4; S^0(HD) and S^0(D$_2$),

H. L. Johnston and E. A. Long, *J. Chem. Phys.*, **2**, 389 (1934); S^0(D$^-$) was calculated at 298 K to be 28.04 cal/deg mol; D^0(NH$_2$–D) was calculated from D^0(NH$_2$–H) and from the difference in the stretching zero point energies: "Tables of Molecular Vibrational Frequencies", Part 1, NSRDS-NBS 6, 1967; S^0(ND$_3$) and S^0(ND$_2^-$) were calculated to be 48.33 and 46.0 cal/deg mol, respectively, at 298 K; the electron affinity of ND$_2$ was assumed to equal that of NH$_2$.
(30) R. D. Levine and R. B. Bernstein, *J. Chem. Phys.*, **56**, 2281 (1972).
(31) R. D. Present, "Kinetic Theory of Gases", McGraw-Hill, New York, N.Y., 1958, Chapter 8.
(32) E. F. Greene and A. Kuppermann, *J. Chem. Educ.*, **45**, 361 (1968).
(33) P. Kebarle in ref 1, p 459.
(34) J. J. Solomon, M. Meot-Ner, and F. H. Field, *J. Am. Chem. Soc.*, **96**, 3727 (1974).
(35) (a) R. Wolfgang, *Acc. Chem. Res.*, **3**, 48 (1970); (b) Z. Herman and R. Wolfgang in ref 16a, pp 591–595.

Crystal Structure of η⁵-Pentamethylcyclopentadienyltriphenylphosphineethylenerhodium(I). A Case of Important π Component in a Metal–Olefin Bond

W. Porzio and M. Zocchi*

Contribution from Istituto di Chimica delle Macromolecole del CNR, 20133 Milano, Italy, and Istituto di Chimica Industriale del Politecnico, Sezione di Strutturistica, 20133 Milano, Italy. Received June 1, 1977

Abstract: The crystal and molecular structure of (η⁵-C₅Me₅)(PPh₃)Rh(C₂H₄) was determined from x-ray intensity data measured by a single-crystal automated diffractometer. Crystals are monoclinic, space group $P2_1/n$, with $a = 12.180$ (1), $b = 23.416$ (2), $c = 9.177$ (1) Å, $\beta = 96.60$ (2)°. The structure was solved by Patterson and Fourier methods and refined by least squares to a conventional R value of 0.037, based on 2359 observed reflections. In the molecule, of approximate C_s symmetry, the rhodium atom is coordinated to a C₅Me₅ ring, a triphenylphosphine molecule, and the ethylene ligand, with the approximate mirror plane passing through the Rh and P atoms and the middle point of the ethylene C–C bond. The geometry of the C₅Me₅ ligand is discussed also with reference to a partial localization of electron charge within the ring. The ethylene ligand, whose hydrogen atoms were clearly located in a Fourier difference map, is far from being planar and its conformation, which is characterized by a twist of 20° of the CH₂ groups about the C–C bond axis and by an almost tetrahedral geometry of the C atoms, suggests an important π component in the metal–ethylene bond.

The Chatt-Dewar description of the bonding between transition metals and olefins is now well accepted in the case of square-planar complexes of low oxidation state transition metals. However, this model, while being qualitatively successful in many other cases, does not give a satisfactory interpretation to the bonding mode in general. In the case of some Rh(I) complexes NMR spectra indicate that rotation of the olefinic ligand about the olefin–metal bond occurs at room temperature,[1,2] thus implying a small or negligible π component in the bond.

A few crystal structures containing molecules with metal-olefin bonds have been solved by Guggenberger et al.;[3–5] in the rhodium complex (η⁵-C₅H₅)Rh(C₂F₄)(C₂H₄)[3] the hydrogen atoms of the ethylenic ligand have been clearly located, showing a coordination geometry essentially identical with the one in the Zeise's salt, with the implication that also in this case the π component is not important.[6]

It seemed useful to us to solve and refine the crystal structure of the title compound, since it offered, in view of its similarity with (η⁵-C₅H₅)Rh(C₂F₄)(C₂H₄), the possibility of studying the influence of other ligands in determining the balance of the σ and π components in the metal-olefin bond. In this context, of particular interest appeared to be the high basicity of triphenylphosphine and the presence of the methyl substituents in the cyclopentadienyl ring, both factors suggesting a relatively important π component in this case, with a significant

electron back-donation from the metal and the establishment of a strong metal–olefin bond.

Experimental Section

Crystals suitable for x-ray diffraction measurements were obtained by crystallization from pentane of a product obtained by reacting (η⁵-C₅Me₅)(PPh₃)RhI₂ and (CH₂)₄MgBr₂[7]. The working conditions of the experiment, carried out on a Philips PW 1100 automatic four-circle diffractometer, and the crystal data are given in Table I.

The unit cell parameters and the space group symmetry were determined using the standard control program of the PW 1100 system,[8] with a randomly oriented crystal. The cell parameters were refined by least squares, using the 2θ values of the reflections belonging to the $h00$, $0k0$, $00l$, and $h0h$ reciprocal lattice rows.

Intensity data were corrected for Lorentz and polarization effects but not for absorption, in view of the small crystal size and absorption coefficient (μ). The atomic positions were determined by the heavy-atom method and refined by least squares, minimizing $\Sigma w(F_o - F_c)^2$ with unitary weight factors, in the block-diagonal approximation.[9] The atomic scattering factors given by Cromer and Mann[10] were used; for the rhodium atom both the real and imaginary dispersion corrections[11] were taken into account.

The thermal vibration parameters were refined isotropically in a first stage (three cycles) and then anisotropically (three more cycles); at the end of this process, involving only the nonhydrogen atoms, the conventional R factor ($R = (\Sigma |KF_o - |F_c||)/\Sigma KF_o$) reached a value of 0.057 calculated on the basis of the 2359 observed reflections. At this point a Fourier difference map was calculated (with $F_o - F_c$